# Spatial Extent of Wave Functions of Gate-Induced Hole Carriers in Pentacene Field-Effect Devices as Investigated by Electron Spin Resonance

Kazuhiro Marumoto,[1,*] Shin-ichi Kuroda,[1] Taishi Takenobu,[2,3] and Yoshihiro Iwasa[2,3]

[1]*Department of Applied Physics, Nagoya University, Nagoya 464-8603, Japan*
[2]*Institute for Materials Research, Tohoku University, Sendai 980-8577, Japan*
[3]*CREST, Japan Science and Technology Corporation, Kawaguchi 332-0012, Japan*

(Received 24 March 2006; published 22 December 2006)

An electron spin resonance (ESR) method is applied to a pentacene field-effect device to investigate gate-induced hole carriers in such devices. Clear field-induced ESR signals are observed, demonstrating that all of the field-injected carriers have $S = 1/2$ spins. Anisotropic ESR signals due to unpaired $\pi$ electrons show the molecular orientation at the interface in the devices. The spatial extent of the spin density distribution (wave function) of the carriers is evaluated from the ESR linewidth, accounting for the hyperfine structure, to be of the order of 10 molecules.

DOI: 10.1103/PhysRevLett.97.256603 PACS numbers: 85.30.Tv, 76.30.−v

Organic materials have applications in low-cost molecular electronic devices such as electroluminescent diodes [1] and field-effect transistors (FETs) [2]. Electroluminescent diodes are currently used in full-color displays, and organic FETs are also approaching the threshold of wide commercial application, with analogous applications to inorganic transistors [1–3]. To improve the performance of organic FETs, it is essential to clarify the intrinsic electronic states of the charge carriers at the interface between the organic and insulating layers [2–4]. In organic FETs, charge carriers accumulate in active organic layers at the interface; the thickness of the active layers is believed to be between one and several monolayers [2–5]. The upper limit of the microscopic carrier mobility in organic crystals falls between 1 and 10 $cm^2\,V^{-1}\,s^{-1}$ [2,4]. This limit has been ascribed to weak intermolecular interactions in organic semiconductors, typically van der Waals interactions, since the vibration energy of molecules is close to the intermolecular bonding energies at or above room temperature [2].

The organic molecule studied in this work is pentacene [see Fig. 1(a)], which is one of the most widely studied organic semiconductors for organic FETs [2]. Field-effect carrier mobilities in pentacene FETs are close to 1 $cm^2\,V^{-1}\,s^{-1}$, and the transport mechanism is considered to be thermally activated hopping [2,4]. Recently, band-transport features have been discussed for highly ordered thin films and single crystals of pentacene [6,7]. In hopping models, the wave function of a carrier is considered to be localized in one molecule [2,4]. In band models, on the other hand, the wave function of a carrier is spatially extended over several molecules [2,4]. The detailed intrinsic properties of the charge carriers in pentacene FETs tend to be masked by extrinsic bulk effects such as FET grain boundaries [2,4–6], and, hence, the microscopic properties of the carrier states have not been completely clarified to date.

In this Letter, we introduce a new method for studying FET structures using electron spin resonance (ESR) and investigate the microscopic properties of charge carriers in pentacene devices. The ESR method can analyze the electronic states of carriers with spins; in particular, it can measure the spin density distribution (wave function) of paramagnetic carriers. It can also be used to measure the molecular orientation by observing the anisotropic $g$ value and linewidth of the ESR signal due to hyperfine coupling of the $\pi$ electrons [8,9]. In applying the ESR method to a field-effect device, we can selectively observe and investigate field-injected carriers and the orientation of molecules where carriers are injected at the interface [10,11]. This field-induced ESR method does not suffer the above-mentioned extrinsic bulk effects. Using this method, we have successfully demonstrated that all field-injected carriers have $S = 1/2$ spin and have evaluated the spin density distribution of carriers to be of the order of 10 molecules.

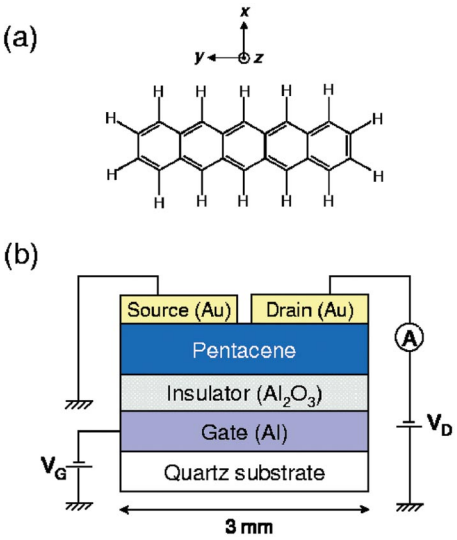


FIG. 1 (color). (a) Chemical structure of pentacene. The principal axes of the proton hyperfine coupling of the $\pi$ electrons are shown. (b) Schematic of the FET structure used in this study. The channel length ($L$) and width ($W$) of the Au source and drain electrodes are 100 $\mu$m and 2.17 cm, respectively.

 

Such a direct observation of the spin states of carriers in organic FETs has not previously been reported.

In our experiments, we used the same device to measure the dependence of the capacitance ($C$) and the FET and ESR characteristics on the gate voltage ($V_G$), with no uncertainty in the reproducibility due to device quality. Figure 1(b) shows a schematic illustration of the pentacene FET structure used in this study. The pentacene was purchased from Aldrich Chemical. A quartz substrate, $3 \times 30$ mm$^2$ in size, was inserted into the ESR sample tube with an inner diameter of 3.5 mm. The substrate and the $Al_2O_3$ gate insulator exhibit no ESR signals [10,11]. An Al gate and Au electrodes were vapor deposited using an ULVAC VPC-250K1 vacuum evaporation system. An $Al_2O_3$ layer with a thickness of ~300 nm was deposited by rf sputtering using an ULVAC AJA ST-20 rf-sputtering gun. A layer of pentacene with a thickness of ~400 nm was vapor deposited using a Sanyu Electron SVC-700TM/700-2 thermal evaporation system. The grain size of the pentacene film was confirmed to be ~0.5 $\mu$m by atomic force microscope.

We consider first the standard operation of the pentacene FET. Figure 2 shows the dependence of $C$ on $V_G$ of the pentacene FET, measured using a Hioki 3511-50 LCR meter equipped with a Hioki 9268 dc bias voltage unit. The source and drain electrodes are short-circuited and grounded, forming a metal-insulator-semiconductor (MIS) diode structure. The active capacitive area was 0.43 cm$^2$. When a negative bias is applied to the Al-gate electrode, $C$ increases as the absolute value of the negative bias increases and plateaus at ~3.7 nF below $\sim -5$ V, owing to the accumulation of positive carriers (holes) at the interface between the $p$-type semiconductor pentacene and the insulator. In the positive-bias region, $C$ shows a low value plateau of ~2.1 nF, owing to the depletion of positive carriers. These capacitance characteristics are similar to those of MIS diodes reported by other groups [12–15]. The inset in Fig. 2 shows the dependence of the drain current $I_D$ on the drain voltage $V_D$ at different $V_G$ values. These transfer characteristics were measured using an Agilent Technology E5270 semiconductor parameter analyzer. The FET characteristic of the $p$-type semiconductor is confirmed by observing the increase in $I_D$ for negative $V_G$. Clear saturation behavior at higher $V_D$ demonstrates standard FET operation. We have evaluated a field-effect mobility $\mu$ of $1.1 \times 10^{-2}$ cm$^2$ V$^{-1}$ s$^{-1}$, a threshold voltage $V_{\text{th}}$ of $6 \times 10^{-5}$ V, and an on-to-off current ratio $>10^2$ for a fixed $V_D$ of $-5$ V in the saturation regime using $I_D = (W/2L)\mu C(V_G - V_{\text{th}})^2$.

We next consider the field-induced ESR signal of pentacene. As stated above, the source and drain electrodes are short-circuited and grounded, forming an MIS diode structure with no lateral applied field between these electrodes. ESR measurements were performed with a Bruker E500 $X$-band spectrometer equipped with an Oxford ESR900 gas-flow cryostat. The field-induced ESR signal is obtained by subtracting the signal at 0 V from that at $V_G < 0$, to account for hole-carrier accumulation. Figure 3 shows the data at $V_G = -30$ V with an external magnetic field $H$ parallel to the substrate. The $g$ value is $2.0024 \pm 0.0001$, and the peak-to-peak linewidth ($\Delta H_{\text{pp}}$) is $1.9 \pm 0.2$ G. At $V_G = 0$ V, no ESR signal due to pentacene was observed, consistent with the fact that undoped pentacene has no ESR signal [16]. The transient response of the field-induced ESR intensity upon application of $V_G$ shows a prompt response, indicating that the ESR signal is due to field-injected hole carriers. Upon applying $V_G$, the ESR intensity increases abruptly and then saturates. When $V_G$ is turned off, the intensity decreases abruptly to its value before $V_G$ was applied. The response time is <20 ms. For short times, observation is difficult due to the signal-to-noise ratio of the ESR system. The line shape of the ESR signal is almost

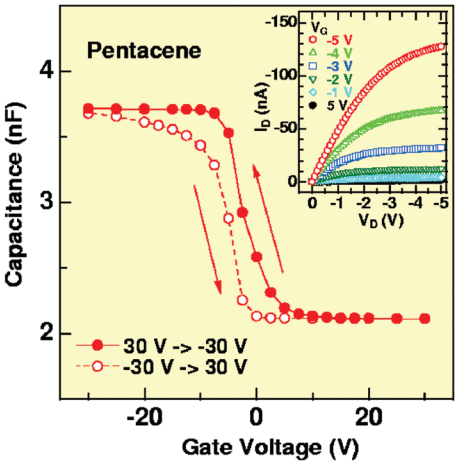


FIG. 2 (color). Gate voltage $V_G$ dependence of capacitance $C$ of pentacene FET structure at a modulation frequency of 120 Hz at 290 K. Inset: Drain current ($I_D$) versus drain voltage ($V_D$) at different $V_G$ for FET at 290 K.

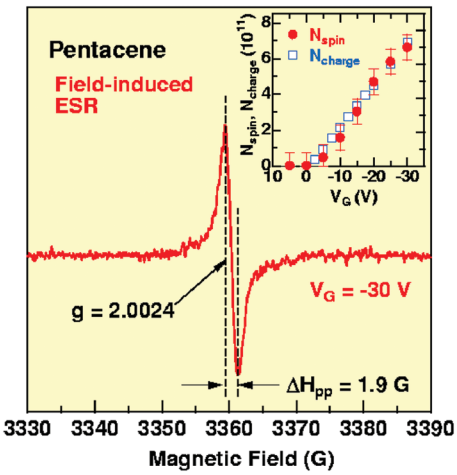


FIG. 3 (color). Field-induced ESR signal of pentacene at 290 K. The external magnetic field is parallel to the substrate. Inset: $V_G$ dependence of the number of field-induced spins $N_{\text{spin}}$ (solid circles) and the number of field-induced charges $N_{\text{charge}}$ (open squares) at 290 K.

Gaussian, as confirmed by the ESR signal for $H$ perpendicular to the plane, shown later in Fig. 4(b). It is also found that $\Delta H_{pp}$ is almost independent of the temperature between 150 and 300 K. The line shape result and the temperature independence of $\Delta H_{pp}$ indicate that the carriers are almost static without motional narrowing of $\Delta H_{pp}$; that is, the carriers exhibit no lateral movement. $\Delta H_{pp}$ is independent of the gate voltage or carrier concentration, which demonstrates that the narrowing of $\Delta H_{pp}$ is not due to spin exchange between neighboring spins.

We obtained the number of field-induced spins $N_{spin}$ from the field-induced ESR signal at various $V_G$. $N_{spin}$ is obtained from the spin susceptibility $\chi$ assuming the Curie law; $\chi$ is obtained by twice integrating the first-derivative ESR signal. The absolute intensity of the ESR signals was calibrated using crystals of $CuSO_4 \cdot 5H_2O$ as a standard. The inset in Fig. 3 shows the dependence of $N_{spin}$ on $V_G$ (solid circles). $N_{spin}$ monotonically increases as the absolute value of $V_G$ increases and reaches $6.6 \times 10^{11}$ (with a density of $1.5 \times 10^{12}$ cm$^{-2}$) at $V_G = -30$ V. The number of field-induced charge carriers $N_{charge}$ (open squares in the inset in Fig. 3) is obtained from $Q = C(|V_G| - V_{th})$, where $Q$ is the charge. $N_{charge}$ monotonically increases as the absolute value of $V_G$ increases and reaches $6.9 \times 10^{11}$ ($1.6 \times 10^{12}$ cm$^{-2}$) at $V_G = -30$ V. $N_{spin}$ and $N_{charge}$ agree very well with each other, which directly demonstrates that all of the field-injected carriers have $S = 1/2$ spins. Note that the static carriers observed by MIS-ESR are the same carrier species as those observed to move in FET channels; the present MIS diode shows FET operation without short-circuiting of the source and drain, as shown in Fig. 2.

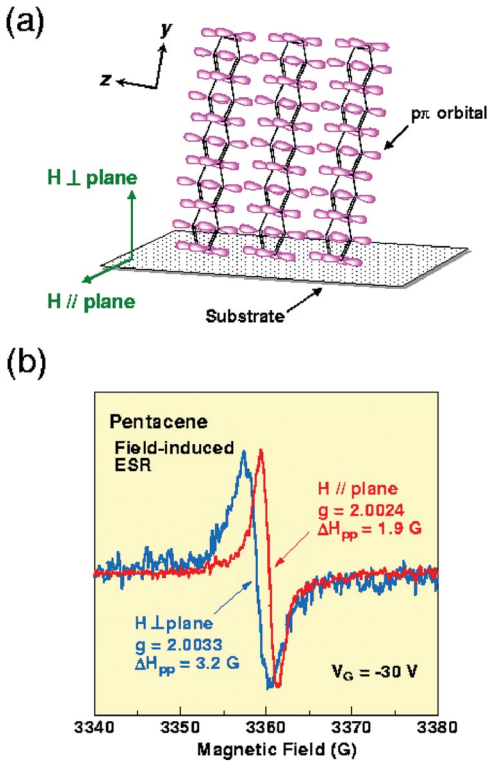


FIG. 4 (color). (a) Schematic diagram of molecular orientation of pentacene in an FET. The $z$ axis is parallel to the $p\pi$ orbital, and the $y$ axis is perpendicular to the $p\pi$ orbital and the C-H bond [see Fig. 1(a)]. (b) Anisotropy of the $g$ values and the linewidth of the field-induced ESR signals for an external magnetic field parallel ($H_\parallel$) and perpendicular ($H_\perp$) to the substrate at 290 K.

We next explain the origin of $\Delta H_{pp}$ by confirming the anisotropy of the field-induced ESR signal reflecting the molecular orientation of pentacene. The averaged molecular orientation for pentacene thin films vapor deposited on substrates of insulating layers is schematically shown in Fig. 4(a), as measured by x-ray diffraction, where the long axis of the molecule is almost perpendicular to the substrate [2,17]. We have confirmed this orientation by our own independent x-ray diffraction measurements. We define the coordinate system of the $p\pi$ orbital in Figs. 1(a) and 4(a) such that the $z$ axis is parallel to the $p\pi$ orbital and the $y$ axis is perpendicular to the $p\pi$ orbital and the C-H bond. The $g$ value of the $\pi$ electron shows nearly uniaxial anisotropy around the $p\pi$-orbital axis: $g_z < g_x \approx g_y$ [8,18]. The origin of $\Delta H_{pp}$ of the $\pi$ electron is the hyperfine coupling between the finite spin density $\rho$ of the carbon $p\pi$ orbital and the proton bounded to the carbon. The magnitude of the hyperfine coupling is $\rho \boldsymbol{A}$, where $\boldsymbol{A}$ is the hyperfine tensor of a $\pi$ electron due to the C-H proton [8–11]. $\boldsymbol{A}$ is diagonal in the above coordinate system, with principal components $A_{xx} = -(1-\alpha)A$, $A_{yy} = -(1+\alpha)A$, and $A_{zz} = -A$ [8–11], where $A$ is McConnell's constant with a magnitude of 56–84 MHz in frequency units, and $\alpha \sim 0.5$ represents the relative magnitude of the anisotropic coupling. Figure 4(b) presents the ESR signals due to field-induced carriers in the device for $H$ parallel ($H_\parallel$) and perpendicular ($H_\perp$) to the substrate, showing a clear anisotropy. The $g$ value for $H_\parallel$ is 2.0024 and for $H_\perp$ is 2.0033. $\Delta H_{pp}$ for $H_\parallel$ is $\Delta H_{pp}^{\parallel} = 1.9$ G and for $H_\perp$ is $\Delta H_{pp}^{\perp} = 3.2$ G. These values show monotonic angular dependence, which is confirmed by observing the values at intermediate angles between $H_\parallel$ and $H_\perp$. The $g$ value and $\Delta H_{pp}$ show a minimum at $H_\parallel$ and a maximum at $H_\perp$. Note that the $g$ value and $\Delta H_{pp}$ at $H_\parallel$ are averaged values due to all possible in-plane molecular orientations in the herringbone arrangement of the molecules in the film; that is, the $x$ and $z$ components are almost averaged at $H_\parallel$, whereas the $y$ component is almost observed at $H_\perp$. The observed anisotropy is well explained by the anisotropy of the tensor components of the $g$ value ($g_z < g_{x,y}$) and the hyperfine coupling ($|A_{yy}| > |A_{zz}| > |A_{xx}|$) [8–11]. That is, the smallest $g_z$ among the $g$-tensor components is almost confined in the film plane, giving a minimum $g$ at $H_\parallel$, whereas the $y$ axis with maximum $|A_{yy}|$ is almost perpendicular to the substrate plane, giving a maximum $\Delta H_{pp}$ at $H_\perp$ [see Fig. 4(a)]. Hence, we have successfully confirmed the molecular orientation of penta-

cene where charge carriers are injected at the interface in the device.

Finally, we discuss the spatial extent of the spin density distribution (wave function) of hole carriers in a pentacene field-effect device, determined from the magnitude of the ESR linewidth. In general, the statistical distribution of hyperfine lines due to many protons within the envelope of a wave function produces an unresolved ESR linewidth. If the protons are simply equivalent to $n$ spins, where $n$ is the number of protons, it is well known that the hyperfine structure tends to follow the binomial distribution, and the half linewidth of the envelope of the ESR signal is then proportional to $\sqrt{n}A_n$ or $(1/\sqrt{n})A_1$, where $A_n$ and $A_1$ are the hyperfine constants for $n$ protons and one proton, respectively, and $A_n = A_1/n$ [19]. In practice, the real wave function gives the distribution of the spin density $\rho$, resulting in inequivalent hyperfine splittings. However, when $n$ is large, $(1/\sqrt{n})A_1$ almost holds [8], as explained below. In the following, we evaluate the spatial extent of $\rho$ of carriers in a field-effect device. To evaluate the spatial extent in the unit of monomers, the ESR linewidth of monomeric pentacene is required. The hyperfine splitting of monomeric pentacene has been reported for the ESR of pentacene cations in the liquid state [20]. With 14 protons in the pentacene monomer, the ESR spectrum shows overlapped hyperfine structures with a full width at half maximum of the envelope of $10 \pm 1$ G [20]. To apply this to the ESR linewidth in the solid state, we must consider the anisotropic part of the hyperfine coupling, which is absent in the liquid state. The contribution of the anisotropic term in randomly oriented ESR tends to wash out the resolved hyperfine structure due to isotropic coupling, giving an envelope linewidth that is nearly identical with that of isotropic coupling [8]. Thus, we adopt the above value of $10 \pm 1$ G as the averaged monomer linewidth in the following discussion.

Considering the statistical distribution of the hyperfine lines [8,19], the linewidth narrows when $\rho$ extends over $N$ molecules as $\Delta H_{\mathrm{pp}} \propto 1/\sqrt{N}$. Let $\rho(1, i)$ be the spin density distribution of a pentacene cation (one molecule), let $i$ be the carbon site of pentacene ($i = 1$–$22$), let $\rho(j, i)$ be the spin density distribution of a hole carrier in a pentacene FET (of $N$ molecules), and let $j$ be the pentacene molecule number ($j = 1 - N$). Then $1 = \sum_i \rho(1, i) = \sum_{j,i} \rho(j, i)$. Using the averaged values, the above equation is modified as $\langle \rho(j, i) \rangle_{\mathrm{av}} = \frac{1}{N} \langle \rho(1, i) \rangle_{\mathrm{av}}$. On the other hand, the linewidth is proportional to $\rho$ as $\Delta H_{\mathrm{pp}} \propto \sqrt{N} \langle \rho(j, i) \rangle_{\mathrm{av}}$ due to the statistical distribution of the hyperfine lines—or the random-walk nature—in other words, similar to the case of the equivalent spins mentioned above [19]. Thus, $\Delta H_{\mathrm{pp}}$ narrows when $N$ is large, as $\Delta H_{\mathrm{pp}} \propto \frac{1}{\sqrt{N}} \langle \rho(1, i) \rangle_{\mathrm{av}}$, where $\langle \rho(1, i) \rangle_{\mathrm{av}}$ is constant. Therefore, $N$ can be evaluated by comparing the linewidths of monomeric pentacene and the pentacene FET. For the pentacene FET, the averaged $\Delta H_{\mathrm{pp}}$ ($\Delta H_{\mathrm{pp}}^{\mathrm{av}} = 2.4$ G) is obtained from the anisotropic $\Delta H_{\mathrm{pp}}$, using $\Delta H_{\mathrm{pp}}^{\mathrm{av}} = \sqrt{[2(\Delta H_{\mathrm{pp}}^{\parallel})^2 + (\Delta H_{\mathrm{pp}}^{\perp})^2]/3}$. Using this value (2.4 G) and the above linewidth of monomeric pentacene (10 G), $N$ in the pentacene FET is evaluated using $\Delta H_{\mathrm{pp}} \propto 1/\sqrt{N}$ as $(10/2.4)^2 \approx 17$, i.e., the order of 10 molecules. This is a notable result, because $N$ in pentacene films has been traditionally taken to be about one molecule, based on the experimental result that thermally hopping features of carrier transport are usually observed in films [2,4,6]. This larger spatial extent of wave functions of gate-induced hole carriers in pentacene FET microscopically supports the recent transport results of pentacene showing band-transport features [6,7]. Other examples of band-transport features have been recently reported for single crystals of rubrene [21,22], and, thus, rubrene seems an interesting subject for future studies. On the basis of the present results, further theoretical investigations into the spatial extent of carriers in organic materials would be useful for understanding organic materials and to assist in improving the performance of organic devices.

This work was supported by Grants-in-Aid for Scientific Research (18686002, 17340094, and 17067007) from the Ministry of Education, Culture, Sports, Science and Technology of Japan.

*Present address: Institute of Materials Science, University of Tsukuba, Tsukuba 305-8573, Japan.
Electronic address: marumoto@ims.tsukuba.ac.jp

[1] R. H. Friend *et al.*, Nature (London) **397**, 121 (1999).
[2] C. D. Dimitrakopoulos and P. R. L. Malenfant, Adv. Mater. **14**, 99 (2002).
[3] E. J. Meijer *et al.*, Nat. Mater. **2**, 678 (2003).
[4] M. Pope and C. E. Swenberg, *Electronic Processes in Organic Crystals and Polymers* (Oxford University Press, Oxford, 1999).
[5] M. Kiguchi *et al.*, Jpn. J. Appl. Phys. **42**, L1408 (2003).
[6] S. F. Nelson *et al.*, Appl. Phys. Lett. **72**, 1854 (1998).
[7] O. D. Jurchescu, J. Baas, and T. T. M. Plastra, Appl. Phys. Lett. **84**, 3061 (2004).
[8] S. Kuroda, Int. J. Mod. Phys. B **9**, 221 (1995).
[9] K. Marumoto, N. Takeuchi, and S. Kuroda, Chem. Phys. Lett. **382**, 541 (2003).
[10] K. Marumoto *et al.*, J. Phys. Soc. Jpn. **73**, 1673 (2004).
[11] K. Marumoto *et al.*, J. Phys. Soc. Jpn. **74**, 3066 (2005).
[12] A. R. Brown *et al.*, Synth. Met. **88**, 37 (1997).
[13] P. J. Brown *et al.*, Phys. Rev. B **63**, 125204 (2001).
[14] S. Scheinert and W. Schliefke, Synth. Met. **139**, 501 (2003).
[15] Y. Furukawa *et al.*, Macromol. Symp. **205**, 9 (2004).
[16] T. Mori and S. Ikehata, Mater. Sci. Eng. B **49**, 251 (1997).
[17] T. Minakata, I. Nagoya, and M. Ozaki, J. Appl. Phys. **69**, 7354 (1991).
[18] J. R. Morton, Chem. Rev. **64**, 453 (1964).
[19] S. Geschwind, *Electron Paramagnetic Resonance* (Plenum, New York, 1972).
[20] J. R. Bolton, J. Chem. Phys. **46**, 408 (1967).
[21] V. Podzorov *et al.*, Phys. Rev. Lett. **95**, 226601 (2005).
[22] J. Takeya *et al.*, Jpn. J. Appl. Phys. **44**, L1393 (2005).